Benign Hepatocellular Nodules: Hepatobiliary Phase of Gadoxetic Acid–enhanced MR Imaging Based on Molecular Background[1]

Norihide Yoneda, MD, PhD
Osamu Matsui, MD, PhD
Azusa Kitao, MD, PhD
Kazuto Kozaka, MD, PhD
Satoshi Kobayashi, MD, PhD
Motoko Sasaki, MD, PhD
Kotaro Yoshida, MD, PhD
Dai Inoue, MD, PhD
Tetsuya Minami, MD, PhD
Toshifumi Gabata, MD, PhD

Gadoxetic acid is a contrast agent for magnetic resonance (MR) imaging with hepatocyte-specific properties and is becoming increasingly important in detection and characterization of hepatocellular carcinoma and benign hepatocellular nodules, including focal nodular hyperplasia (FNH), nodular regenerative hyperplasia (NRH), hepatocellular adenoma (HCA), and dysplastic nodule. In these hepatocellular nodules, a positive correlation between the grade of membranous uptake transporter organic anion–transporting polypeptide (OATP) 1B3 expression and signal intensity in the hepatobiliary (HB) phase has been verified. In addition, it has been clarified that OATP1B3 expression is regulated by activation of β-catenin and/or hepatocyte nuclear factor 4α. On the other hand, recent studies have also revealed some of the background molecular mechanisms of benign hepatocellular nodules. FNH commonly shows iso- or hyperintensity in the HB phase with equal or stronger OATP1B3 expression, with map-like distribution of glutamine synthetase (a target of Wnt/β-catenin signaling) and OATP1B3 expression. NRH shows doughnut-like enhancement with hypointensity in the central portion in the HB phase with OATP1B3 expression. The majority of HCAs show hypointensity in the HB phase, but β-catenin–activated HCA exclusively demonstrates iso- or hyperintensity with increased expression of nuclear β-catenin, glutamine synthetase, and OATP1B3. Dysplastic nodule commonly shows iso- or hyperintensity in the HB phase with similar to increased OATP1B3 expression, but one-third of high-grade dysplastic nodules can be demonstrated as a hypointense nodule with decreased OATP1B3 expression. Knowledge of these background molecular mechanisms of gadoxetic acid–enhanced MR imaging is important not only for precise imaging diagnosis but also understanding of the pathogenesis of benign hepatocellular nodules.

Abbreviations: B-HCA = β-catenin–activated HCA, FNH = focal nodular hyperplasia, HB = hepatobiliary, HCA = hepatocellular adenoma, HCC = hepatocellular carcinoma, H-HCA = HNF-1α–inactivated HCA, HNF = hepatocyte nuclear factor, I-HCA = inflammatory HCA, NRH = nodular regenerative hyperplasia, OATP = organic anion–transporting polypeptide, SAA-HN = serum amyloid A–positive hepatocellular neoplasm

RadioGraphics 2016; 36:0000–0000

Published online 10.1148/rg.2016160037

Content Codes: GI MR OI

[1]From the Departments of Radiology (N.Y., O.M., A.K., K.K., K.Y., D.I., T.M., T.G.), Quantum Medical Imaging (S.K.), and Human Pathology (M.S.), Kanazawa University Graduate School of Medical Science, 13-1 Takaramachi, Kanazawa, Ishikawa 920-8640, Japan. Recipient of a Magna Cum Laude award for an education exhibit at the 2015 RSNA Annual Meeting. Received March 3, 2016; revision requested May 18 and received June 9; accepted July 12. For this journal-based SA-CME activity, the authors, editor, and reviewers have disclosed no relevant relationships. **Address correspondence to** N.Y. (e-mail: *noritin@f7.dion.ne.jp*, *noritiny@staff.kanazawa-u.ac.jp*).

SA-CME LEARNING OBJECTIVES

After completing this journal-based SA-CME activity, participants will be able to:

- Describe the molecular background of benign hepatocellular nodules.
- List the imaging findings of benign hepatocellular nodules, especially in the HB phase of gadoxetic acid–enhanced MR imaging.
- Discuss the differential diagnosis of benign hepatocellular nodules.

See www.rsna.org/education/search/RG.

Introduction

Gadoxetic acid (gadolinium ethoxybenzyl diethylenetriaminepentaacetic acid; Gd-EOB-DTPA; Primovist, Bayer Schering Pharma, Berlin, Germany) is a contrast agent for magnetic resonance (MR) imaging with hepatocyte-specific properties (1,2). Around 50% of intravenously injected gadoxetic acid is taken up by hepatocytes and then excreted into the bile ducts and the other half into urine rapidly (1). In the hepatobiliary (HB) phase around 20 minutes after intravenous injection of gadoxetic acid, the liver parenchyma is strongly enhanced, resulting in clear visualization of mass lesions (which commonly do not take up gadoxetic acid) as definite hypointense nodules. In addition, gadoxetic acid can be used in the same way as gadopentetate dimeglumine to evaluate the hemodynamics of hepatic lesions in the dynamic phase.

TEACHING POINTS

- In addition to HCCs, it has been verified that HCA, FNH, and dysplastic nodule also show a significant correlation between signal intensity in the HB phase of gadoxetic acid–enhanced MR imaging and OATP1B3 expression in their constitutional cells. On the basis of these reports, OATP1B3 is considered to be the main uptake transporter of gadoxetic acid in hepatocellular nodules determining the signal intensity in the HB phase.
- The majority of FNHs show iso- or hyperintensity in the HB phase of gadoxetic acid–enhanced MR imaging relative to the surrounding liver with equal or stronger OATP1B3 expression compared with that of background liver. Grazioli et al reported that 62 of 68 FNHs (91%) were iso- or hyperintense in the HB phase. Not rarely, FNH shows ring or doughnut-like enhancement due to relative hypointensity in the peri–central scar area in the HB phase due to relatively lower expression of OATP1B3 in the hyperplastic hepatocytes surrounding the central scar.
- In NRH, HB phase images from gadoxetic acid–enhanced MR imaging show doughnut-like enhancement with relative hypointensity in the central portion. The central relatively hypointense portion corresponds to the central portal tracts and surrounding hyperplastic hepatocytes. In our experience, OATP1B3 is commonly overexpressed in NRH.
- Importantly, the majority of B-HCAs show iso/hyperintensity in the HB phase of gadoxetic acid–enhanced MR imaging, with overexpression of OATP1B3 and glutamine synthetase and occasional intranuclear β-catenin expression.
- Around one-third of high-grade dysplastic nodules showed slightly decreased OATP1B3 expression; all other high-grade dysplastic nodules and low-grade dysplastic nodules demonstrated OATP1B3 expression similar to or higher than that of the surrounding liver. Because of this OATP1B3 expression, both low- and high-grade dysplastic nodules commonly show iso-/hyperintensity relative to the surrounding liver in the HB phase, but one-third of high-grade dysplastic nodules can be demonstrated as a faintly hypointense nodule.

Because of these features, gadoxetic acid–enhanced MR imaging has been proved to have higher sensitivity in detection of hepatocellular carcinoma (HCC) than dynamic computed tomography (CT) and gadopentetate dimeglu ine–enhanced MR imaging and to provide better diagnostic accuracy than dynamic CT for differentiation of hepatic mass lesions (3–6). As a result, gadoxetic acid–enhanced MR imaging is becoming increasingly important in detection and characterization of hepatic mass lesions, including not only HCC and other malignant neoplasms but also benign hepatocellular nodules.

Hepatic nodules are divided into four types according to their origin: hepatocyte, cholangiocyte, mesenchymal cell, and others. Among them, some of the hepatocellular nodules, not only hyperplastic nodules but also some hepatocellular adenomas (HCAs) and HCCs, can take up larger amounts of gadoxetic acid, resulting in iso/hyperintensity relative to the surrounding liver in the HB phase (7–11). In these hepatocellular nodules, a positive correlation between the expression grade of sinusoidal membranous uptake transporter organic anion–transporting polypeptide (OATP) 1B3 (synonymous with OATP8) and enhancement ratio in the HB phase has been verified (7,8,10–13).

Table 1: Benign Hepatocellular Nodules Originating from Hepatocytes

Focal nodular hyperplasia (FNH)
FNH
FNH-like nodule
Serum amyloid A–positive hepatocellular neoplasm (SAA-HN)
Nodular regenerative hyperplasia (NRH)
Hepatocellular adenoma (HCA)
HNF-1α–inactivated HCA (H-HCA)
Inflammatory HCA (I-HCA)
β-catenin–activated HCA (B-HCA)
Unclassified HCA
Dysplastic nodule

Note.—HNF = hepatocyte nuclear factor.

In addition, the molecular/genetic background of OATP1B3 expression in HCC cells has been elucidated (14–18). On the other hand, recent studies have also revealed some of the background molecular mechanisms of benign hepatocellular nodules, particularly HCA with subtype classification and focal nodular hyperplasia (FNH) (19–21). To know them in relation to the HB phase findings and OATP1B3 expression is useful not only for image interpretation but also for understanding the pathogenesis of benign hepatocellular nodules.

The aim of this article is to review the molecular background of hepatocellular benign nodules, namely FNH, nodular regenerative hyperplasia (NRH), HCA, and dysplastic nodule (Table 1), and to correlate the findings in the HB phase of gadoxetic acid–enhanced MR imaging with the molecular background.

This review article focuses on the following topics: *(a)* epidemiology, cause, pathologic and clinical features; *(b)* molecular/genetic background; and *(c)* imaging findings and correlation between HB phase findings and molecular background in benign hepatocellular nodules. The differential diagnosis among benign hepatocellular nodules and from HCC is also described.

Surmised Molecular/Genetic Mechanisms of OATP1B3 Expression Analyzed in HCCs

In rat hepatocytes, sinusoidal membranous OATP1 was confirmed to be an uptake trans-

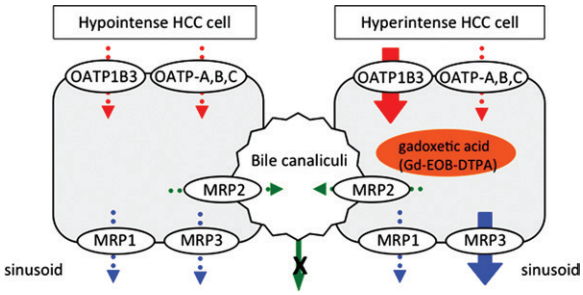

Figure 1. Supposed mechanism of transportation of gadoxetic acid in human HCC. In HCCs showing hypointensity in the HB phase of gadoxetic acid–enhanced MR imaging, the uptake of gadoxetic acid is reduced because of decreased expression (dotted arrows) of OATP1B3 relative to the surrounding liver. In contrast, in HCCs showing hyperintensity in the HB phase, gadoxetic acid is taken up from sinusoids into HCC cells by increased expression (solid arrows) of OATP1B3 and excreted into blood sinusoids again by MRP3. The influence of the excretion transporter on the signal intensity of HCC in the HB phase around 20 minutes after intravenous injection may be minimal, because the function of MRP2 may be blocked due to the depletion of bile ducts in HCCs, and the excretion again into tumor blood sinusoids by MRP3 may be gradual. Therefore, the signal intensity (enhancement ratio) of HCCs in the HB phase reflects the grade of OATP1B3 expression. *Gd-EOB-DTPA* = gadolinium ethoxybenzyl diethylenetriaminepentaacetic acid. (Adapted and reprinted, with permission, from reference 8.)

porter of gadoxetic acid (22) and multidrug-resistance protein (MRP) 2, which is expressed on the canalicular side as an export transporter (23). In human hepatocytes, regarding export transporters, rat MRP2 is a homologue to human MRP2, which is expressed on the canalicular side. In addition, MRP3 and MRP1 on the sinusoidal side can export some of the substrates of MRP2 into blood compensatorily when the function of MRP2 is disturbed (24). Concerning the uptake transporters, the human OATP group including OATP1B1 and OATP1B3 are now considered to be the main functioning players (25,26).

After the introduction of gadoxetic acid–enhanced MR imaging into clinical practice, it soon became clear that around 10%–15% of hypervascular classic HCCs showed iso- or hyperintensity relative to the surrounding liver in the HB phase (paradoxical enhancement) (7,8,27). Narita et al (7) and Kitao et al (8) analyzed the expression of these transporters quantitatively by Western blot or polymerase chain reaction methods in HCCs and showed a correlation between the enhancement ratio of HCCs in the HB phase and grade of OATP1B3 expression in HCC cells. This indicated that OATP1B3 expression in HCC cells determines the signal intensity of HCC in the HB phase (7,8) (Fig 1).

The influence of the excretion transporter on the signal intensity of HCC in the HB phase around 20 minutes after intravenous injection is considered to be minimal, because the function of MRP2 may be blocked due to the depletion of bile ducts in HCCs, and the excretion again into tumor blood sinusoids by MRP3 may be gradual. In addition to HCCs, it has been verified that HCA, FNH, and dysplastic nodule also show a significant correlation between signal intensity in the HB phase of gadoxetic acid–enhanced MR imaging and OATP1B3 expression in their constitutional cells (8,10–13,28). On the basis of these reports, OATP1B3 is considered to be the main uptake transporter of gadoxetic acid in hepatocellular nodules determining the signal intensity in the HB phase.

Further molecular and genetic analyses in HCCs have revealed that HCC showing hyperintensity in the HB phase (OATP1B3-overexpressed HCC) is a peculiar subtype of HCC with a biologically less aggressive nature and molecular/genetic features of mature hepatocytes with β-catenin and hepatocyte nuclear factor (HNF) 4α activation (17,18).

In normal liver parenchyma, β-catenin is known to regulate the expression of genes related to xenobiotic metabolism including cytochrome p450, glutamine synthetase, and OATPs in pericentral (zone 3) hepatocytes (Fig 2) (29–31). Interestingly, Colletti et al (32) reported the convergence of Wnt/β-catenin signaling on the HNF-4α–driven transcription-controlled liver-zonated gene expression in an experimental study (Fig 3). A similar molecular mechanism of OATP1B3 expression in HCCs and other hepatocellular nodules can be expected.

Focal Nodular Hyperplasia

Epidemiology, Cause, Pathologic and Clinical Features

FNH is the second most common benign liver tumor after hemangioma with a prevalence of 0.9%. It is seen most commonly in women aged 20–50 years (male-to-female ratio = 1:8) (34). It commonly occurs in normal liver parenchyma as a solitary nodule (80%) and often occurs near the surface of the liver. Some FNHs are related to vascular disease, such as hereditary hemorrhagic telangiectasia or congenital absence of the portal vein (35,36). One study reported that FNH is not hormonally dependent (37). FNH is considered a benign hyperplastic lesion due to a perfusion disorder (38).

The gross appearance of representative FNH consists of lobulated contours. FNH is composed of hyperplastic hepatocytes without atypia arranged in one- to two-cell-thick plates. The central scar is a characteristic finding in FNH. The central scar usually contains fibrous tissue, numerous small arterioles, and dystrophic vessels connected to surrounding hepatic venules. Ductular proliferation is often observed in the

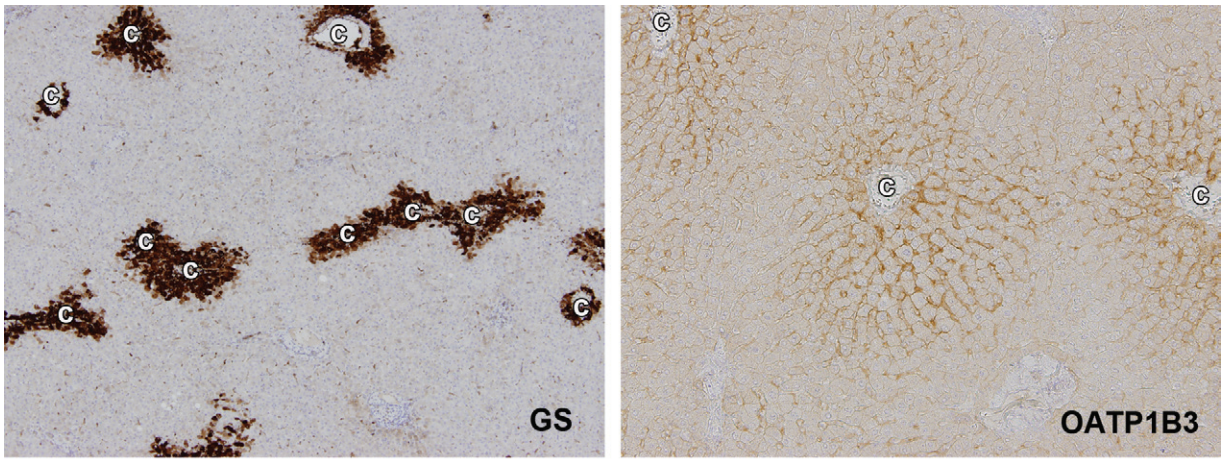

a. b.

Figure 2. Expression of glutamine synthetase and OATP1B3 in pericentral (zone 3) hepatocytes in the liver. Immunohistochemical staining for glutamine synthetase *(GS)* **(a)** and OATP1B3 **(b)** shows their expression in pericentral (zone 3) hepatocytes in the normal liver as dark (glutamine synthetase) or light (OATP1B3) brown staining. *C* = central vein. (Original magnification, ×40.)

scar lesion (39). An internal portal vein and mature bile ducts are commonly absent in FNH.

Most cases of FNH are asymptomatic without the risks of hemorrhage or malignant transformation (40). Therefore, basically no treatment is needed. FNH remains stable or may even decrease in size at follow-up.

Molecular/Genetic Background

No somatic gene mutations in the β-catenin gene *(CTNNB1)*, *TP53*, *APC*, or *HNF1α* have been identified by genetic analysis in FNH (19,41,42). Dysregulation of the angiopoietin genes (*ANGPT1* and *ANGPT2*), which are responsible for maturation of blood vessels, has been reported (19,43). In a recent study, FNH showed activation of the Wnt/β-catenin pathway without any mutations in the gene encoding β-catenin *(CTNNB1)* or Axin1 mutation like HCA (44).

Activation of glutamine synthetase, which is one of the major downstream targets of β-catenin, and its perivenous map-like distribution indicating polyclonal proliferation of hepatocytes were observed in FNH (45). This map-like distribution of glutamine synthetase is almost diagnostic for FNH (45). Regarding the uptake transporter of gadoxetic acid, equal or stronger OATP1B3 expression compared with that of background liver is seen and its distribution is map-like, consistent with glutamine synthetase expression (Fig 4) (13,46).

Imaging Findings and Correlation of HB Phase Findings with Molecular Background

The majority of FNHs show iso- or hyperintensity in the HB phase of gadoxetic acid–enhanced MR imaging relative to the surrounding liver with

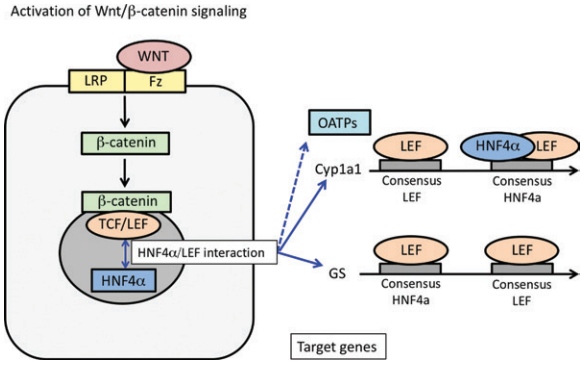

Figure 3. Surmised molecular mechanism of the expression of genes related to xenobiotic metabolism in pericentral-type hepatocytes. Activation of Wnt/β-catenin signaling is seen in the pericentral-type hepatocytes. In the nucleus, β-catenin activates the T-cell factor *(TCF)*/lymphoid enhancer factor *(LEF)* class, and LEF interacts with HNF-4α. Then, glutamine synthetase *(GS)* and cytochrome *(Cyp)* 1a1 are expressed as some of the target genes. OATPs may be expressed by the same mechanism as Cyp, because OATPs and Cyps show decreased expression in HNF-4α–null mice (33). *Fz* = Frizzled receptor, *LRP* = lipoprotein receptor–related protein. (Adapted and reprinted, with permission, from reference 32.)

equal or stronger OATP1B3 expression compared with that of background liver (13,46). Grazioli et al (9) reported that 62 of 68 FNHs (91%) were iso- or hyperintense in the HB phase (Fig 5). Not rarely, FNH shows ring or doughnut-like enhancement due to relative hypointensity in the peri–central scar area in the HB phase due to relatively lower expression of OATP1B3 in the hyperplastic hepatocytes surrounding the central scar (13,46) (Fig 6).

Mohajer et al (47) reported the following three enhancement patterns: type 1 = uniform uptake iso- or hyperintense to liver (59%), type 2 = hyperintense rim with core that is hypointense to liver (9%), type 3 = hyperintense rim

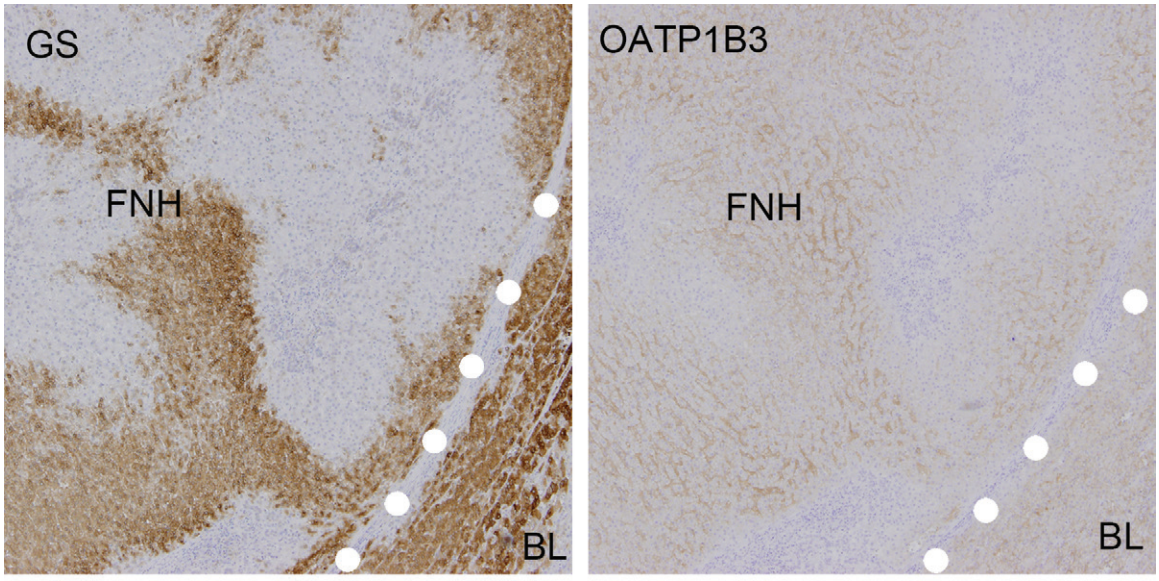

a. b.

Figure 4. Map-like pattern of glutamine synthetase and OATP1B3 expression in FNH. Immunohistochemical staining of the resected specimen for glutamine synthetase *(GS)* **(a)** and OATP1B3 **(b)** shows a broad, anastomosing, map-like distribution as brown staining. The areas of glutamine synthetase and OATP1B3 expression are largely consistent. Map-like distribution of glutamine synthetase is diagnostic for FNH. *BL* = background liver. (Original magnification, ×40.)

a.

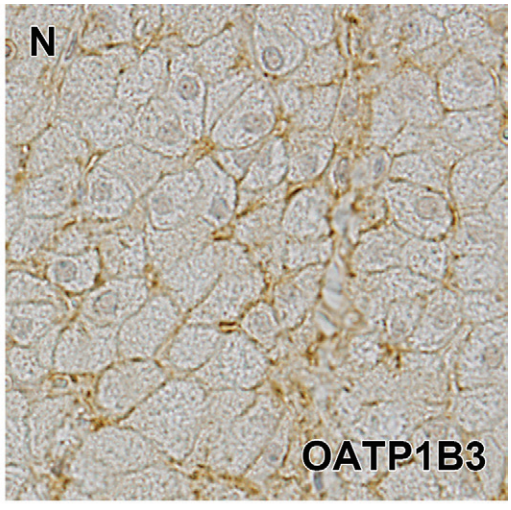

b.

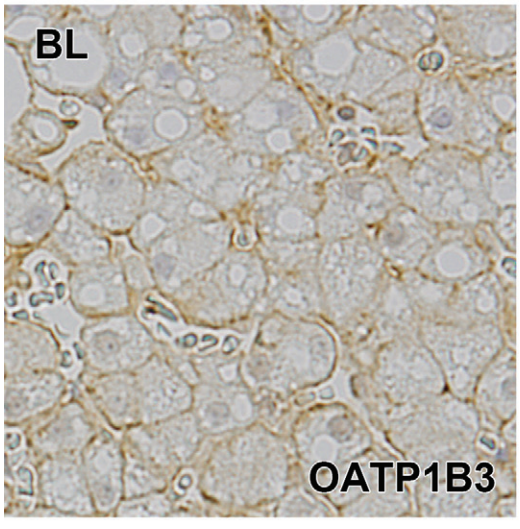

c.

Figure 5. FNH in a 14-year-old girl. **(a)** HB phase gadoxetic acid–enhanced MR image shows an FNH nodule (arrows), which is isointense to surrounding liver with a hypointense central scar (arrowhead). **(b, c)** Immunohistochemical staining for OATP1B3 in a biopsy specimen from the nodule (*N* in **b**) and background liver (*BL* in **c**). OATP1B3 expression in the nodule (brown staining on the sinusoidal side of the membrane) is almost the same as that of background liver. (Original magnification, ×400.)

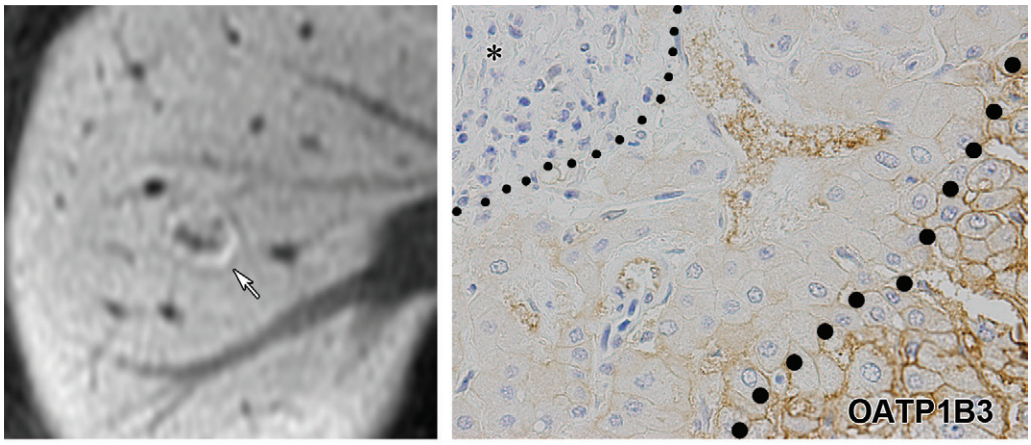

a. b.

Figure 6. Ring or doughnut-like enhancement in FNH. **(a)** FNH in a 41-year-old woman. HB phase gadoxetic acid–enhanced MR image shows ring or doughnut-like enhancement (relative hypointensity in the central portion) (arrow). **(b)** FNH in a 23-year-old man. Immunohistochemical staining for OATP1B3 in the resected specimen shows almost absent expression of OATP1B3 in hyperplastic hepatocytes (between dotted lines) surrounding the central scar (*). There is definite expression of OATP1B3 in the outer hyperplastic hepatocytes, which appears as brown staining. (Original magnification, ×400.)

with core that is iso- or hyperintense to liver (32%). The reason why the hyperplastic hepatocytes surrounding the central scar show relative hypointensity with lower expression of OATP1B3 and glutamine synthetase is unknown. However, it is speculated that the hepatocytes surrounding the central scar may originate from periportal venous (zone 1) hepatocytes and the hepatocytes in the peripheral portion from perivenular (zone 3) hepatocytes. To confirm this further investigation is needed.

FNH-like Nodule in Alcoholic Cirrhosis/SAA-HN

Epidemiology, Cause, Pathologic and Clinical Features

Typical FNH occurs in noncirrhotic liver. On the other hand, FNH-like nodule is a hyperplastic hepatocellular nodule similar to FNH occurring in cirrhotic liver (48,49). This FNH-like nodule is seen especially in alcoholic cirrhosis (48). FNH-like nodule in alcoholic cirrhosis resembles HCC at imaging (50).

Molecular/Genetic Background

Recently, a new approach to diagnosis of FNH-like nodule in alcoholic cirrhosis has emerged based on immunohistochemistry. Recent studies have reported that some FNH-like nodules in alcoholic cirrhosis show histologic features of inflammatory HCA (I-HCA): sinusoidal dilatation, ductular reaction, inflammatory reaction, and strong immunoreactivity for serum amyloid A (SAA). Because HCA generally arises in the absence of significant fibrosis and cirrhosis, this nodule was tentatively named SAA-positive hepatocellular neoplasm (SAA-HN).

Accordingly, classic FNH-like nodules can be divided into two categories: FNH-like nodule and SAA-HN (51,52). SAA-HN has neoplastic features like I-HCA (53). The details of the clinicopathologic differences between SAA-HN and FNH-like nodule are now under investigation. On the other hand, a recent study also supports the existence of I-HCA occurring in cirrhosis (54). Therefore, SAA-HN will be classified as I-HCA in the near future. Further investigation is needed on this issue.

Imaging Findings and Correlation of HB Phase Findings with Molecular Background

Imaging features of FNH-like nodule are basically similar to those of FNH. However, FNH-like nodule and SAA-HN commonly demonstrate arterial enhancement and washout in the delayed phase, resembling HCC (50). They usually show iso- to hyperintense signal on T1-weighted images and varied signal intensity on T2-weighted images. Superparamagnetic iron oxide (SPIO) uptake is often observed in the tumor.

The imaging findings of FNH-like nodule and SAA-HN are usually similar except for the gadoxetic acid–enhanced MR imaging findings. FNH-like nodule shows isointensity in the HB phase with equal expression of OATP1B3 compared with background liver, like FNH (Fig 7). However, Sasaki et al (53) reported that eight of 12 SAA-HNs (67%) showed hypointensity in the HB phase, like I-HCA (Fig 8).

There is a possibility that gadoxetic acid–enhanced MR imaging can allow distinction

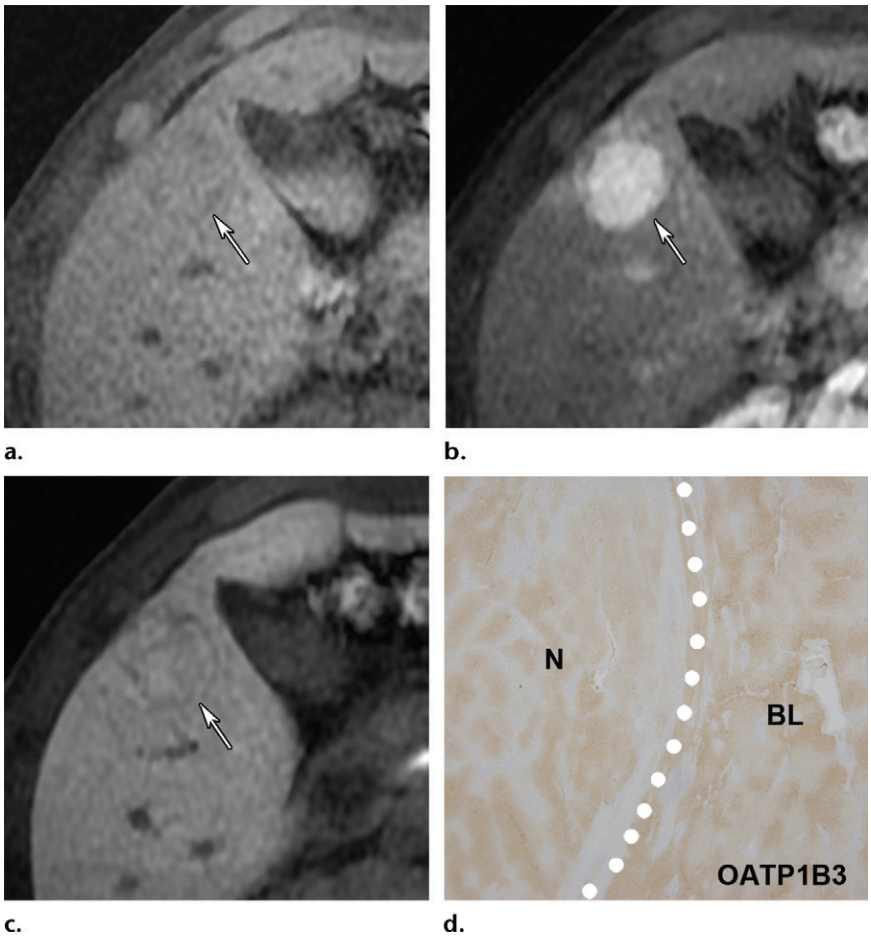

Figure 7. FNH-like nodule in a 48-year-old man with alcoholic cirrhosis. **(a)** Precontrast fat-suppressed T1-weighted MR image shows an FNH-like nodule (arrow) as isointense to surrounding liver. **(b)** Arterial dominant phase gadoxetic acid–enhanced MR image shows enhancement of the nodule (arrow). **(c)** HB phase gadoxetic acid–enhanced MR image shows that the nodule (arrow) is isointense to surrounding liver. **(d)** Immunohistochemical staining of the resected specimen for OATP1B3 shows map-like expression in the nodule *(N)* as brown staining; the grade of expression is similar to that of background liver *(BL)*. Histologically, the tumor was a hepatocellular hyperplastic lesion without atypia, with map-like glutamine synthetase expression and without serum amyloid A expression (not shown). (Original magnification, ×12.5.)

between these two types of hepatocellular benign mass lesion—FNH-like hyperplastic nodule and I-HCA–like neoplastic nodule—occurring in cirrhotic livers. However, further clinical, pathologic, genetic/molecular, and radiologic investigations are needed on this issue.

Nodular Regenerative Hyperplasia

Epidemiology, Cause, Pathologic and Clinical Features

NRH commonly occurs in normal liver parenchyma. The prevalence of NRH was reported to be 2.6% in autopsy series (55). NRH affects males and females equally. It is associated with various diseases (56), such as Budd-Chiari syndrome, myeloproliferative syndromes, collagen vascular disorders, and idiopathic portal hypertension, and with immunosuppressive or antineoplastic medicines. NRH is considered to be a reaction to heterogeneous portal blood flow (55).

Diffuse nodules (1–3 mm in size) are commonly observed, although nodules greater than several centimeters have also been found (55). Unlike in cirrhosis, little or no fibrosis is characteristic of NRH. Sinusoidal dilatation is often seen in NRH. Larger portal veins are commonly seen in the center of the nodule and predominantly supply the entire nodule. This is an important point for understanding the hemodynamics of NRH at imaging. NRH is often asymptomatic, although diffuse NRH is often associated with portal hypertension.

Molecular/Genetic Background

The underlying details of the molecular background are still unclear in NRH. In our experience, NRH cases demonstrate a hepatocellular

Figure 8. SAA-HN in a 44-year-old woman with alcoholic cirrhosis. **(a)** Precontrast fat-suppressed T1-weighted MR image shows an SAA-HN (arrow) as isointense to surrounding liver. **(b)** Arterial dominant phase gadoxetic acid–enhanced MR image shows enhancement of the nodule (arrow). **(c)** HB phase gadoxetic acid–enhanced MR image shows that the nodule (arrow) is slightly hypointense to surrounding liver. **(d, e)** Immunohistochemical staining for OATP1B3 in biopsy specimens from the nodule (*N* in **d**) and background liver (*BL* in **e**) shows faint expression of OATP1B3 as brown staining in the nodule, with weaker expression than that in background liver. Histologically, the tumor was a hepatocellular lesion without marked atypia. Positive serum amyloid A expression was observed (not shown). (Original magnification, ×40.)

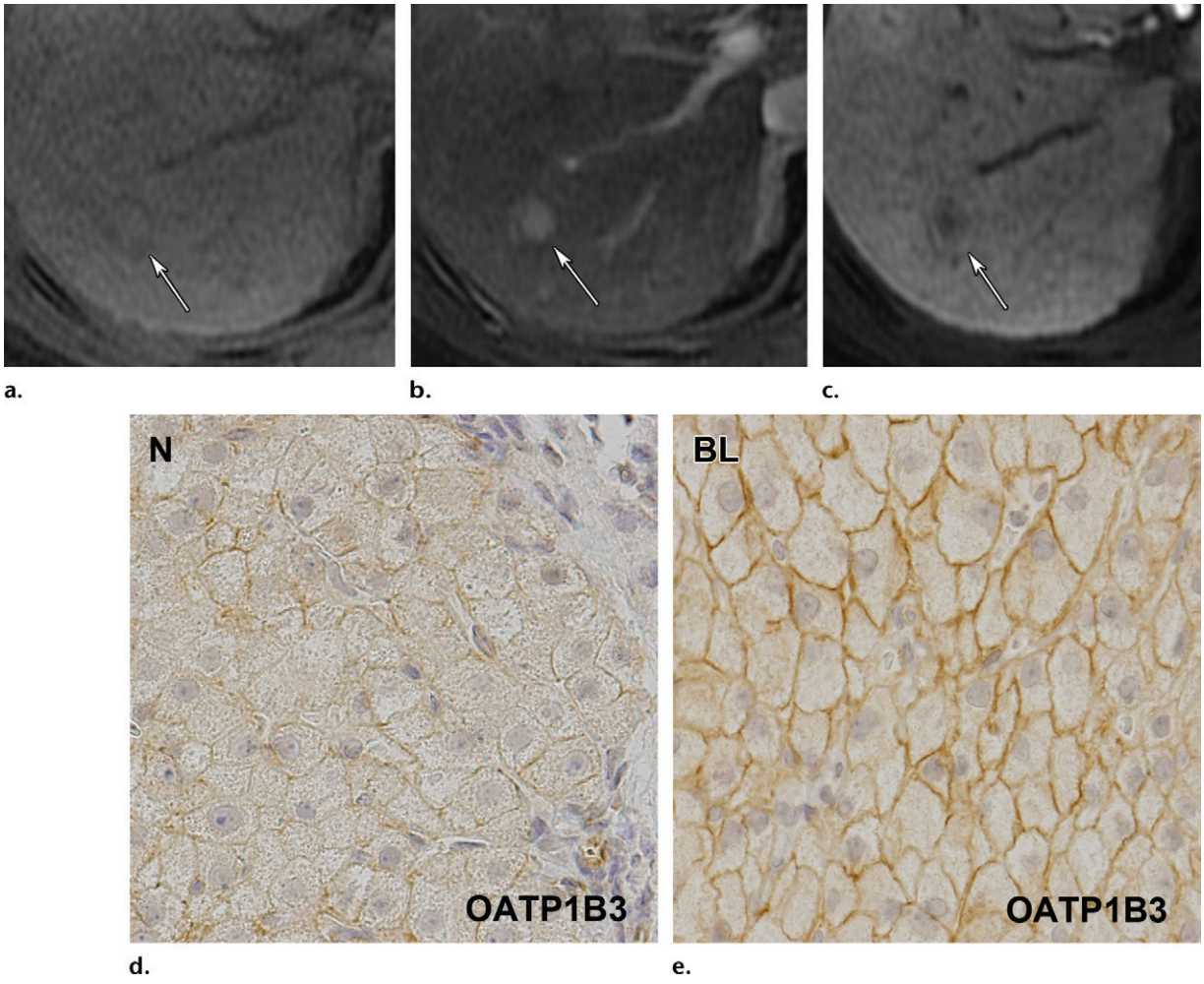

hyperplastic lesion with definite membranous OATP1B3 expression.

Imaging Findings and Correlation of HB Phase Findings with Molecular Background

NRH is supplied by portal blood flow. Therefore, in the arterial dominant phase of dynamic CT and MR imaging, NRH is hypoattenuating/hypointense to background liver, with slight to moderate enhancement in the portal venous phase, becoming isoattenuating/isointense in the equilibrium phase. CT during arterial portography (CTAP) reveals definite enhancement of the entire nodule with contrast material perfusion through the portal venules in the central portion of the nodule.

In NRH, HB phase images from gadoxetic acid–enhanced MR imaging show doughnut-like enhancement with relative hypointensity in the central portion. The central relatively hypointense portion corresponds to the central portal tracts and surrounding hyperplastic hepatocytes (Fig 9). In our experience, OATP1B3 is commonly overexpressed in NRH (Fig 10).

Hepatocellular Adenoma

Epidemiology, Causes, Pathologic and Clinical Features

The prevalence of HCA is three to four per 100 000 persons in Europe and the United States. HCA is rare in Asia (57). Most HCAs occur in young women; they are rare in children, men, and the elderly. HCAs commonly occur in normal liver parenchyma.

Oral contraceptive (58) and androgenic steroid (59) use and hepatic vascular disorders such as Budd-Chiari syndrome and congenital portosys-

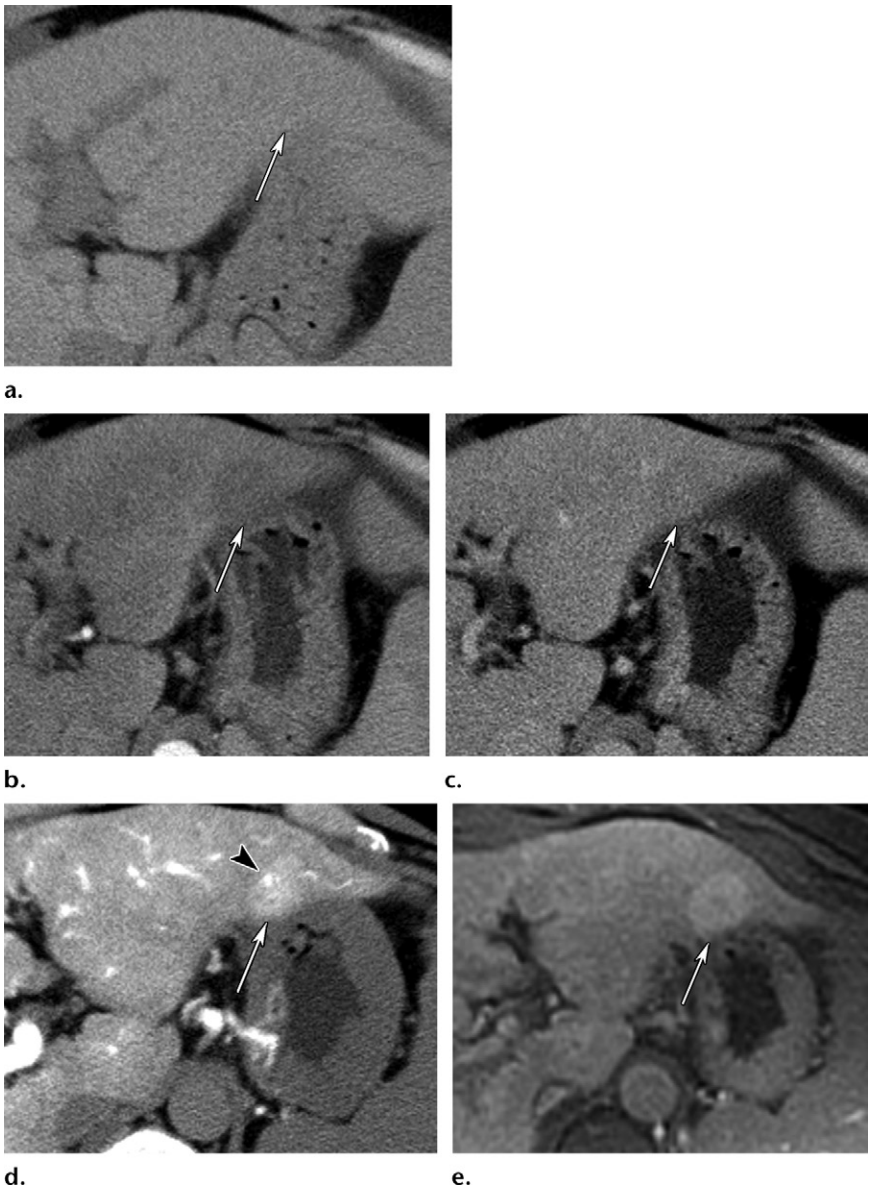

Figure 9. NRH in a 42-year-old woman with idiopathic portal hypertension. **(a)** Precontrast CT image does not show the NRH nodule (arrow), indicating that it is isoattenuating to surrounding liver. **(b)** Arterial dominant phase CT image shows that the nodule (arrow) is hypoattenuating to background liver. **(c)** Delayed phase CT image shows mild internal enhancement of the nodule (arrow). **(d)** CT during arterial portography (CTAP) image shows enhancement of the nodule (arrow) with a portal branch in the central portion (arrowhead). This finding suggests that NRH is supplied by portal blood flow. **(e)** HB phase gadoxetic acid–enhanced MR image shows that the nodule has doughnut-like enhancement (arrow), with hypointensity in the central portion. The hypointense central portion may correspond to a portal tract in the nodule. (Case courtesy of Kouichi Kifune, MD, PhD, Municipal Tsuruga Hospital, Tsuruga, Japan.)

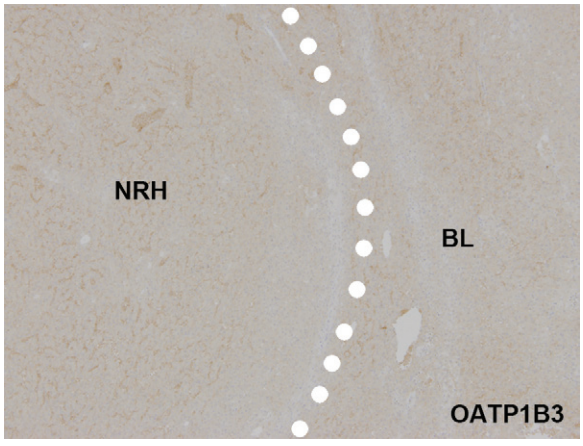

Figure 10. NRH in a 35-year-old woman with idiopathic portal hypertension. Immunohistochemical staining of the resected specimen for OATP1B3 shows membranous OATP1B3 expression in an NRH nodule as brown staining, similar to that of background liver *(BL)*. (Original magnification, ×40.)

temic shunt (60) are well-known risk factors for HCA. HCAs associated with glycogen-storage disease type 1 (von Gierke disease) or type 3 (Forbes disease) are also well known (61,62). A recent study revealed HCAs to be related to maturity-onset diabetes of the young (MODY) type 3 (20). HCA commonly occurs as a solitary mass, rarely as multiple lesions. The presence of more than 10 HCA nodules was termed *adenomatosis* by Flejou et al (63) in 1985.

HCA is composed of benign hepatocytes without nuclear atypia or mitoses (39). HCAs commonly have little or no capsule. HCAs often have internal fat, congestion, necrosis, hemorrhage, or fibrosis. An internal portal tract and cholangiolar proliferation are commonly absent in HCAs (39). Recently, HCAs were divided into four subtypes according to their molecular/genetic and clinical features (20,64,65).

Table 2: Molecular/Genetic/Clinicopathologic Backgrounds of HCA Subtypes

Features	H-HCA	I-HCA	B-HCA	Unclassified HCA
Frequency (%)	35–50	40–55	15–18	10
Gene mutations	*TCF1* (HNF-1α)	*IL6ST* (gp130), *STAT3*, *GNAS*	*CTNNB1* (β-catenin)	...
Immunohistochemistry	L-FABP negative	SAA and CRP positive About 10% have β-catenin mutation	Glutamine synthetase, intranuclear β-catenin, and OATP1B3 positive	...
Clinical features	Occurs mostly in women	Occurs in women and men Obesity and alcohol are risk factors	Occurs mostly in men	...
Pathologic features	Marked steatosis	Inflammatory reaction Ductular reaction Sinusoidal dilatation	Malignant transformation	...

Note.—CRP = C-reactive protein, L-FABP = liver fatty acid–binding protein, SAA = serum amyloid A.

Table 3: Imaging Features of HCA Subtypes

Imaging Features	H-HCA	I-HCA	B-HCA	Unclassified HCA
Typical features	Diffuse signal dropout on out-of-phase T1WI	Hyperintense rim at periphery of lesion on T2WI (atoll sign)	Intralesional scar	...
Hemodynamics	Mild to moderate arterial hypervascularity	Strong arterial hypervascularity	Mild to moderate arterial hypervascularity	Variable
HB phase	Hypointense	Hypointense (some hyperintense)	Iso- or hyperintense	Hypointense

Note.—T1WI = T1-weighted images, T2WI = T2-weighted images.

Patients may have upper quadrant pain and a palpable mass, while up to 50% of patients are asymptomatic. HCAs occasionally bleed, and intraperitoneal hemorrhage can be a fatal complication. Fifteen percent to 20% of HCAs may demonstrate hemorrhage (66). Malignant transformation of HCA to HCC has been reported to occur in about 5%–10% of HCAs (67,68).

HCA Subtypes

HCAs are classified into four subtypes according to their molecular/genetic features: HNF-1α–inactivated HCA (H-HCA), inflammatory HCA (I-HCA), β-catenin–activated HCA (B-HCA), and unclassified HCA (20,64,65). Summaries of the molecular/genetic/clinical-pathologic backgrounds and imaging features of HCA subtypes are provided in Tables 2 and 3, respectively.

HNF-1–inactivated HCA

Epidemiology, Cause, Pathologic and Clinical Features, Molecular/Genetic Background.—H-HCA constitutes 35%–50% of all HCAs. This type predominantly occurs in women who use oral contraceptives. In H-HCA, multiple nodules are often seen.

H-HCA involves mutation of the *TCF1* gene, which encodes HNF-1α. HNF-1α is involved in hepatocyte differentiation (69). Nonfunctioning HNF-1α protein promotes lipogenesis and hepatocellular proliferation. As a result, suppression of liver fatty acid–binding protein (L-FABP) occurs, leading to intracellular fat deposition in H-HCA. Decrease of L-FABP level at immunohistochemistry is a useful diagnostic tool for H-HCA (64,70).

Diffuse fat deposition in the tumor is typical of H-HCA histopathologically. In addition, less cytologic abnormalities and less inflammatory infiltration are also characteristic of H-HCA. H-HCA is a less aggressive subtype compared with other types of HCAs (67). H-HCAs are often associated with maturity-onset diabetes of the young (MODY) type 3 and familial hepatic adenomatosis (20,70).

Imaging Findings and Correlation of HB Phase Findings with Molecular Background.—Regarding the imaging features of H-HCA, diffuse signal

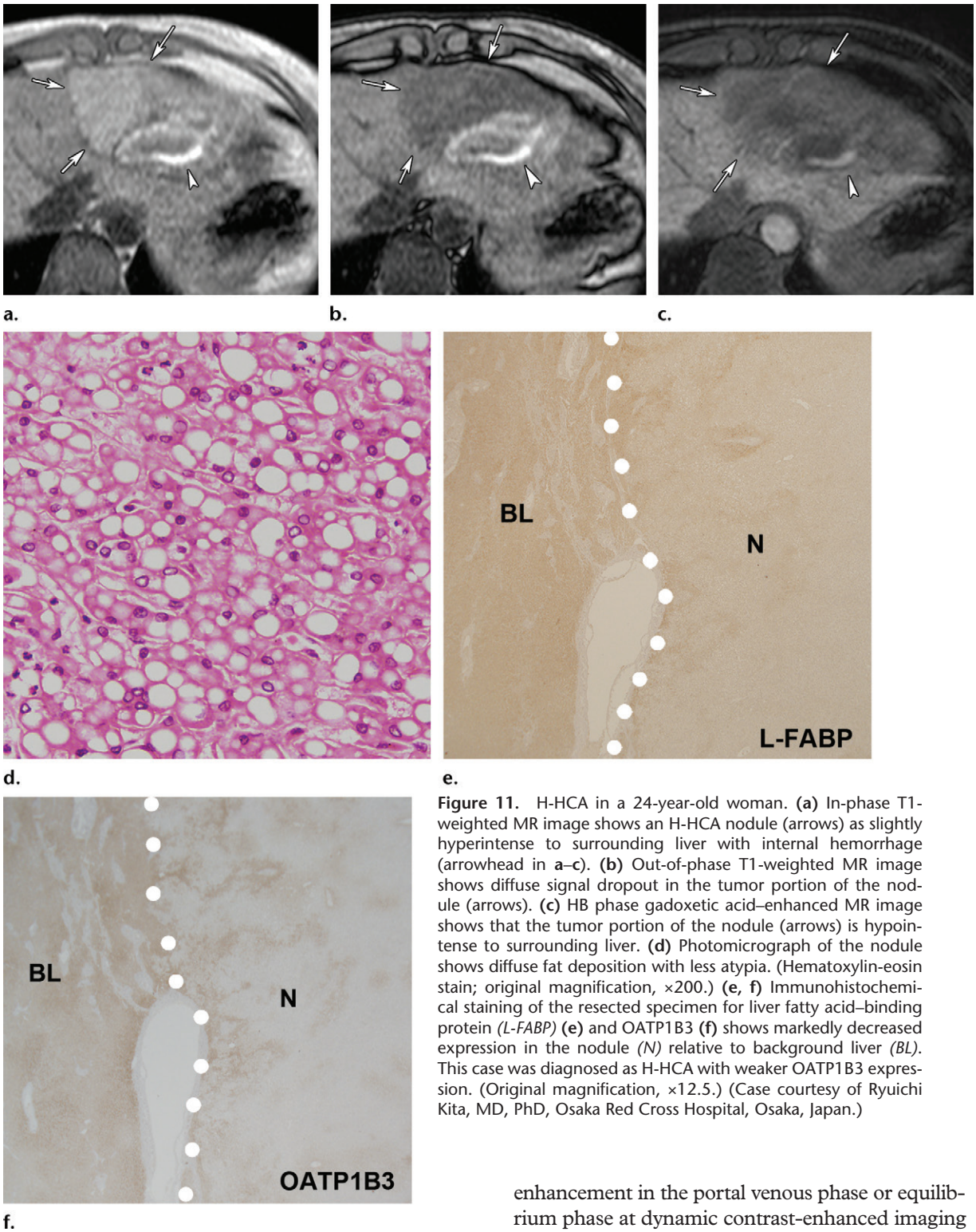

Figure 11. H-HCA in a 24-year-old woman. **(a)** In-phase T1-weighted MR image shows an H-HCA nodule (arrows) as slightly hyperintense to surrounding liver with internal hemorrhage (arrowhead in **a**–**c**). **(b)** Out-of-phase T1-weighted MR image shows diffuse signal dropout in the tumor portion of the nodule (arrows). **(c)** HB phase gadoxetic acid–enhanced MR image shows that the tumor portion of the nodule (arrows) is hypointense to surrounding liver. **(d)** Photomicrograph of the nodule shows diffuse fat deposition with less atypia. (Hematoxylin-eosin stain; original magnification, ×200.) **(e, f)** Immunohistochemical staining of the resected specimen for liver fatty acid–binding protein *(L-FABP)* **(e)** and OATP1B3 **(f)** shows markedly decreased expression in the nodule *(N)* relative to background liver *(BL)*. This case was diagnosed as H-HCA with weaker OATP1B3 expression. (Original magnification, ×12.5.) (Case courtesy of Ryuichi Kita, MD, PhD, Osaka Red Cross Hospital, Osaka, Japan.)

dropout on out-of-phase T1-weighted images due to intracellular steatosis is typical; this has been shown in 78%–93% of H-HCAs (71,72). Iso- to slightly hyperintense signal is seen on T2-weighted images. Internal signal intensity is commonly homogeneous in H-HCA.

There is typically mild to moderate enhancement in the arterial dominant phase, with no persistent enhancement in the portal venous phase or equilibrium phase at dynamic contrast-enhanced imaging (71–73). In the HB phase of gadoxetic acid–enhanced MR imaging, H-HCA exclusively shows hypointensity, with decreased expression of OATP1B3 relative to the surrounding liver (9) (Fig 11).

Inflammatory HCA

Epidemiology, Cause, Pathologic and Clinical Features, Molecular/Genetic Background.— I-HCA is the most common subtype of HCA

Figure 12. I-HCA in a 37-year-old man. **(a)** Precontrast fat-suppressed T1-weighted MR image shows an I-HCA nodule (arrow) as isointense to surrounding liver. **(b)** Arterial dominant phase gadoxetic acid–enhanced MR image shows enhancement of the nodule (arrow). **(c)** HB phase gadoxetic acid–enhanced MR image shows that the nodule (arrow) is hypointense to surrounding liver. **(d)** Immunohistochemical staining of the resected specimen for serum amyloid A *(SAA)* shows diffuse expression of serum amyloid A in the nodule *(N)* as brown staining compared with background liver *(BL)*. **(e)** Immunohistochemical staining for OATP1B3 shows markedly decreased OATP1B3 expression in the nodule *(N)* compared with background liver *(BL)*. (Original magnification in **d** and **e**, ×40.) (Case courtesy of Takehiro Akahane, MD, PhD, Japanese Red Cross Ishinomaki Hospital, Ishinomaki, Japan.)

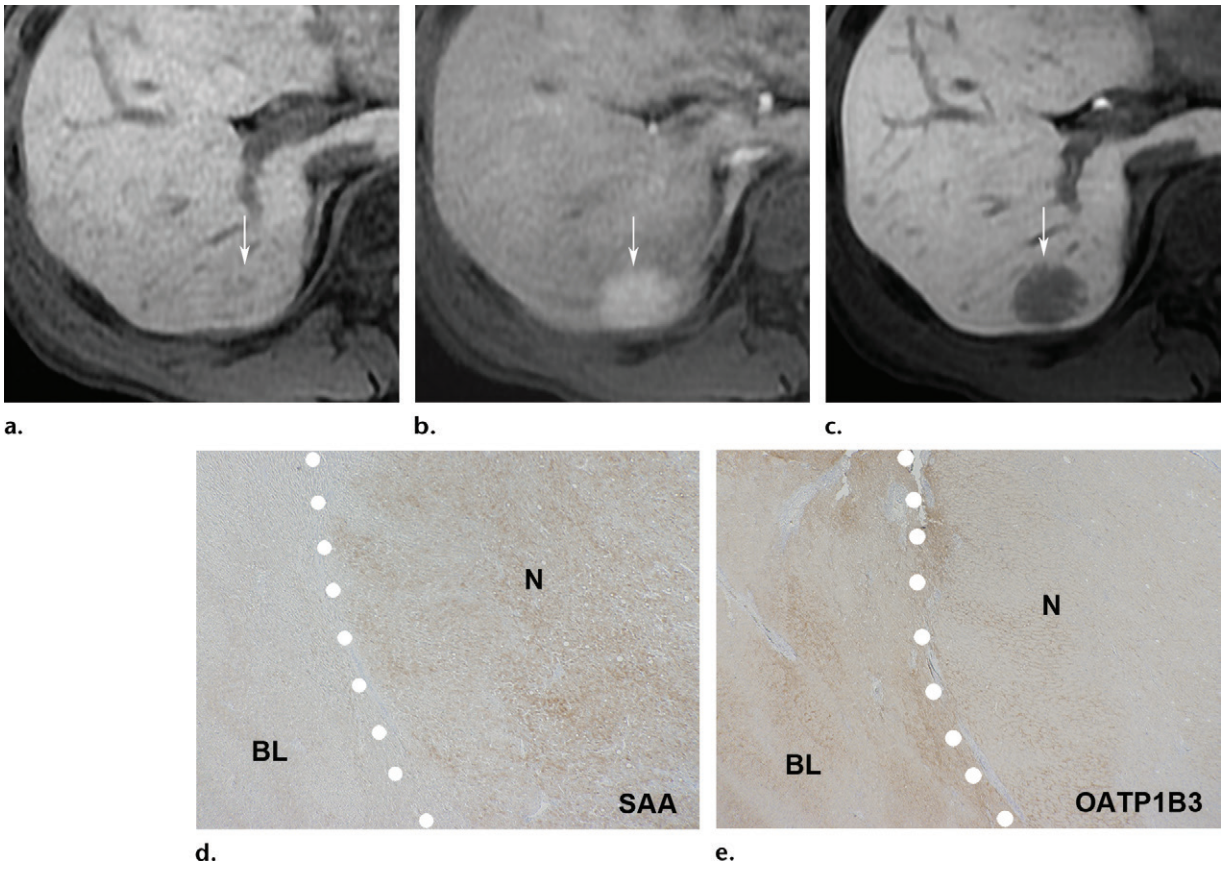

(40%–55%). I-HCAs most commonly occur in young women and sometimes in men (64). Obesity and alcohol intake are risk factors for I-HCA (64). I-HCA patients may have chronic anemia, fever, leukocytosis, and elevated serum C-reactive protein (CRP) (74).

Sustained activation of the Janus kinase (JAK) signal transducer and activation of transcription (STAT) pathway (JAK-STAT pathway) are implicated in the pathogenesis of I-HCA. Sixty percent of I-HCAs have gain-of-function mutation of the *IL6ST* gene, which encodes the oncogene gp130 (75). Several oncogenes such as *IL6ST*, *STAT3*, and *GNAS* have been identified in I-HCA, and their mutations cause activation of the JAK-STAT signaling pathway (75–77).

Activation of acute-phase inflammation proteins, such as serum amyloid A (SAA) and CRP, is often observed in I-HCA. Expression of these inflammation proteins (SAA and CRP) at immunohistochemistry is diagnostic for I-HCA. Previously termed *telangiectatic FNH*, it is now classified as I-HCA (19,64). Approximately 10% of I-HCAs have a β-catenin activation, which is considered to promote their malignant transformation (32,45,64). Pathologically, the presence of inflammatory infiltrates, marked sinusoidal dilatation or congestion, ductular reaction, and numerous thick-walled arteries is characteristic of I-HCA (78).

Imaging Findings and Correlation of HB Phase Findings with Molecular Background.—I-HCA shows hyperintensity on T2-weighted images and iso- to mild hyperintensity on T1-weighted images. A hyperintense rim along the periphery of the lesion on T2-weighted images is considered to be due to dilated sinusoids uniquely seen in I-HCA and is referred to as the atoll sign (71). The atoll sign can be seen in about 40% of I-HCAs (72). At dynamic study, strong arterial enhancement is a typical finding of I-HCA. Persistent enhancement in the portal venous phase and equilibrium phase is also reported as a characteristic finding (71). Focal microscopic fat may be seen (72).

I-HCA commonly shows hypointensity compared with the background liver in the HB phase

of gadoxetic acid–enhanced MR imaging (Fig 12) (9). However, in a recent study some I-HCAs demonstrated hyperintense signal in the HB phase (79). Because β-catenin–activated HCA (B-HCA) exclusively shows iso- or hyperintensity in the HB phase as described later (10,11), it is speculated that I-HCA with β-catenin activation/mutation—which can be seen in approximately 10% of I-HCAs—might show hyperintensity. To confirm this further study is needed.

β-Catenin–activated HCA

Epidemiology, Cause, Pathologic and Clinical Features, Molecular/Genetic Background.—B-HCAs constitute 15%–18% of all HCAs. This type of HCA occurs more frequently in men compared with the other types of HCA. β-catenin is encoded by the catenin b1 gene *(CTNNB1)*. β-catenin mutation results in sustained activation of β-catenin protein, resulting in uncontrolled hepatocyte proliferation. Glutamine synthetase and OATP1B3, which are downstream targets of the Wnt/β-catenin pathway (Fig 3), are diffusely positive in B-HCA but show no map-like distribution like in FNH (32).

At pathologic analysis, the presence of cytologic abnormalities and an acinar pattern are characteristic. B-HCA has potential for malignant transformation (70). This is a very important feature of B-HCA clinically. B-HCA is often associated with glycogen-storage disease and familial adenomatous polyposis (65).

Imaging Findings and Correlation of HB Phase Findings with Molecular Background.—B-HCA shows heterogeneous signal intensity on T2-weighted images and commonly contains no intratumoral steatosis. Slight to moderate arterial hypervascularity is observed in B-HCA (72). van Aalten et al (72) reported internal scars in around 75% of B-HCAs. Importantly, the majority of B-HCAs show iso/hyperintensity in the HB phase of gadoxetic acid–enhanced MR imaging, with overexpression of OATP1B3 and glutamine synthetase and occasional intranuclear β-catenin expression (Fig 13) (10,11).

Unclassified HCA

About 10% of HCAs are classified as unclassified HCA. No *HNF-1α*, *CTNNB1*, or *IL6ST* mutations are identified in unclassified HCA. The underlying molecular pathways/mechanisms remain unclear. No specific imaging findings have been reported. van Aalten et al (72) reported five unclassified HCAs with no steatosis in the lesion and hemorrhagic components in three (60%). Grazioli et al (9) reported that six of eight unclassified HCAs showed hypointensity in the HB phase of gadoxetic acid–enhanced MR imaging.

Dysplastic Nodule

Epidemiology, Cause, Pathologic and Clinical Features

Dysplastic nodules are usually detected in cirrhotic livers or chronically damaged liver. At gross examination, they appear as single or multiple nodules with distinct or indistinct margins and internal portal tracts. Most dysplastic nodules are less than 15 mm in diameter. Dysplastic nodules are classified as low grade or high grade depending on the degree of atypia (80). High-grade dysplastic nodules have clonal features, are categorized as a premalignant lesion, and demonstrate frequent progression to HCC. In some cases, iron or copper accumulation or steatosis is observed. Dysplastic nodules are mainly supplied from portal veins; sporadic unpaired arteries can be seen (81).

Molecular/Genetic Background, Imaging Findings, and Correlation of HB Phase Findings with Molecular Background

A recent study revealed significant decline of OATP1B3 expression from the early stage of multistep hepatocarcinogenesis in accordance with the grade of malignancy of hepatocellular nodules (12). Around one-third of high-grade dysplastic nodules showed slightly decreased OATP1B3 expression; all other high-grade dysplastic nodules and low-grade dysplastic nodules demonstrated OATP1B3 expression similar to or higher than that of the surrounding liver (12). Because of this OATP1B3 expression, both low- and high-grade dysplastic nodules commonly show iso-/hyperintensity relative to surrounding liver in the HB phase, but one-third of high-grade dysplastic nodules can be demonstrated as a faintly hypointense nodule.

Differential Diagnosis among Benign Hepatocellular Nodules

Background liver and imaging features of benign hepatocellular nodules are summarized in Table 4. FNH, NRH, and HCA commonly occur in normal liver. On the other hand, dysplastic nodule, FNH-like nodule, and SAA-HN arise against a background of chronic liver disease.

At imaging, FNH, FNH-like nodule, and SAA-HN usually show arterial enhancement in the arterial dominant phase of dynamic study. On the other hand, NRH and dysplastic nodule demonstrate no definite enhancement in the arterial dominant phase, but show increasing enhancement in the portal/equilibrium phase due to a predominantly

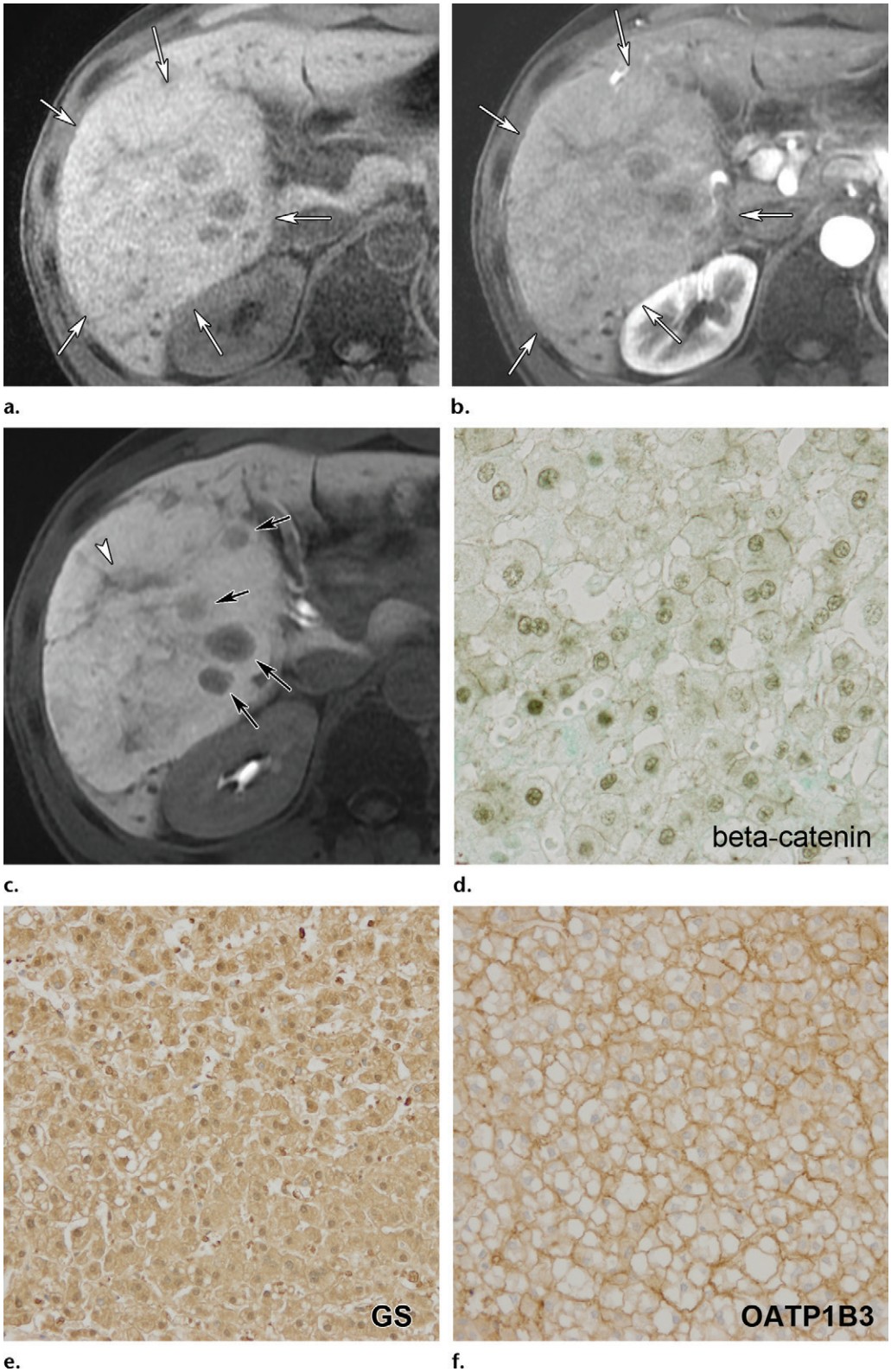

Figure 13. B-HCA in a 31-year-old man. **(a)** Precontrast fat-suppressed T1-weighted MR image shows a B-HCA nodule (arrows) as isointense to surrounding liver. **(b)** Arterial dominant phase gadoxetic acid–enhanced MR image shows heterogeneous faint enhancement of the nodule (arrows). **(c)** HB phase gadoxetic acid–enhanced MR image shows that the nodule is diffusely hyperintense. Several areas of necrosis (arrows) and scar (arrowhead) are seen as hypointense areas. **(d)** Immunohistochemical staining of the resected specimen for β-catenin shows diffuse intranuclear β-catenin expression as dark green staining. (Original magnification, ×400.) **(e, f)** Immunohistochemical staining of the resected specimen for glutamine synthetase **(e)** and OATP1B3 **(f)** shows diffuse cytoplasmic glutamine synthetase *(GS)* expression as brown staining in **e** and diffuse membranous OATP1B3 expression as brown staining in **f**. (Original magnification, ×200.) (Case courtesy of Kiyoshi Murata, MD, PhD, Shiga University of Medical Science, Ōtsu, Japan, and Akira Furukawa, MD, PhD, Tokyo Metropolitan University, Tokyo, Japan.)

Table 4: Background Liver and Imaging Features of Benign Hepatocellular Nodules

Type of Nodule	Background Liver	Sex Predominance	Malignant Potential	Arterial Vascularity	Kupffer Cells	HB Phase	Other Features
FNH	Normal	Female	No	Marked	Yes	Iso- or hyperintense (ring or doughnut enhancement)	Central scar, spoke wheel pattern
FNH-like	Cirrhosis*	Male	No	Marked	Yes	Iso- or hyperintense	...
SAA-HN	Cirrhosis*	Male	Some	Marked	Yes	Hypointense	...
NRH	Normal	None	No	Hypointense†	Yes	Iso- or hyperintense (doughnut enhancement)	...
H-HCA	Normal	Female	No	Mild to moderate	Yes or no	Hypointense	Diffuse fat
I-HCA	Normal	None	Some	Marked	Yes or no	Hypointense‡	Atoll sign
B-HCA	Normal	Male	Yes	Mild to moderate	Yes or no	Iso- or hyperintense	Scar
Dysplastic nodule	Damaged	None	Yes	Iso- or hypointense	Yes	Iso- or hyper- to hypointense	...
HCC	Damaged	None	Malignant	Mild to marked	No	Hypointense§	Mosaic/corona enhancement

*FNH-like nodule and SAA-HN occur especially often in alcoholic cirrhosis.
†NRH is supplied by portal venous flow.
‡Some I-HCAs are iso- to hyperintense in the HB phase.
§About 10% of HCCs are hyperintense in the HB phase.

portal venous supply. FNH, FNH-like nodule, SAA-HN, NRH, and dysplastic nodule usually show preserved intratumoral Kupffer cells. Therefore, differentiation among them by using reticuloendothelial contrast agents is difficult.

At gadoxetic acid–enhanced MR imaging, SAA-HN, H-HCA, and I-HCA usually show hypointensity in the HB phase, except for some I-HCAs that demonstrate iso- or hyperintensity and may have internal β-catenin mutations. On the other hand, FNH, FNH-like nodule, NRH, and B-HCA almost exclusively demonstrate iso- or hyperintensity in the HB phase due to overexpression of OATP1B3.

In FNH, FNH-like nodule, and NRH, doughnut or ring-like peripheral stronger enhancement is often seen, due to the zonation of OATP1B3 expression in these hyperplastic hepatocytes. Dysplastic nodules may show hyper-, iso-, or hypointensity in the HB phase according to the grade of malignancy and OATP1B3 expression during multistep hepatocarcinogenesis. In the imaging differential diagnosis among these hepatocellular benign nodules, understanding these imaging features, especially those at gadoxetic acid–enhanced MR imaging, is helpful in making the correct diagnosis.

Differential Diagnosis of Benign Hepatic Nodules from HCC

Clinically, the differential diagnosis of benign hepatocellular nodules from HCC is most important.

Differential Diagnosis of Hyperintense Benign Nodules in HB Phase from HCC

Around 10%–15% of hypervascular classic HCCs show paradoxical uptake of gadoxetic acid (hyperintense HCC, HCC with OATP1B3 overexpression) (7,8,27). In HCCs with OATP1B3 overexpression, in our experience, pseudocapsule formation and/or internal mosaic architecture is often seen. Differentiation between FNH, NRH, and HCC with OATP1B3 overexpression at imaging is relatively easy according to the imaging features, including hemodynamics and other imaging features as described earlier.

Table 5: Glossary of Molecular Terms in This Article

Term*	Meaning	Related Lesion (Benign)
Transporters		
OATP1B3	Main uptake transporter of gadoxetic acid	FNH, NRH, B-HCA
MRP1, MRP3	Export transporters expressed on sinusoidal side	...
MRP2	Main export transporter of gadoxetic acid expressed on canalicular side	...
Genes		
TCF1	Encodes HNF-1α	H-HCA
IL6ST	Encodes the interleukin 6 receptor gp130	I-HCA
STAT3	Encodes a key nuclear transcription factor that induces the acute-phase inflammatory response	I-HCA
GNAS	Encodes the α-stimulatory subunit of the trimeric guanine nucleotide binding (or G-protein, GSα)	I-HCA
CTNNB1	Encodes β-catenin	B-HCA
Signaling		
JAK-STAT	Activated by binding of interleukin 6 to its cell membrane	I-HCA
Wnt/β-catenin	Related to hepatocarcinogenesis and essential for development and organogenesis	B-HCA
Others		
β-catenin	Regulates cell-cell adhesion and gene transcription	B-HCA
Glutamine synthetase	Key enzyme in nitrogen metabolism, downstream target of Wnt/β-catenin signaling	FNH, B-HCA
SAA	Acute-phase inflammation protein	I-HCA, SAA-HN
L-FABP	Normally expressed at high levels within hepatocyte cytoplasm and involved in fatty acid trafficking	H-HCA
HNF-1α	Transcription factor involved in hepatocyte differentiation	H-HCA

*JAK-STAT = Janus kinase signal transducer and activation of transcription pathway, L-FABP = liver fatty acid–binding protein, MRP = multidrug-resistance protein, SAA = serum amyloid A.

Differentiation between B-HCA and HCC with OATP1B3 overexpression is difficult with imaging alone. Clinical information (eg, age, background liver, tumor markers) is necessary for differential diagnosis. However, because B-HCA has potential for malignant transformation, the clinical management can be similar. When differential diagnosis by imaging in combination with clinical findings is difficult, biopsy is needed.

Differential Diagnosis of Hypointense Benign Nodules in HB Phase from HCC

Differentiation between SAA-HN and HCC with imaging is extremely difficult because SAA-HN occurs in alcoholic damaged liver, and liver biopsy is needed. H-HCA has diffuse fat. Therefore, differentiation from HCC with fatty metamorphosis is difficult at imaging. Clinical information (eg, size change, tumor marker) is important for differential diagnosis. In the case of a liver tumor with diffuse fat in a young woman, H-HCA should always be kept in mind.

As for I-HCA, the atoll sign on T2-weighted images is a useful finding suspicious for I-HCA, although only about 40% of I-HCAs show it. Therefore, clinical information is also important for differential diagnosis. Because the imaging findings of HCCs are extremely variable, differential diagnosis between benign hepatocellular nodules showing hypointensity in the HB phase of gadoxetic acid–enhanced MR imaging and nodular HCCs without a capsule and/or internal mosaic architecture is difficult with imaging alone, and biopsy diagnosis with immunohistochemical analysis is needed.

Conclusion

The signal intensity of various benign hepatocellular nodules in the HB phase of gadoxetic acid–enhanced MR imaging reflects their molecular backgrounds, especially related to OATP1B3 and β-catenin expression and possibly HNF-4α activation in the constitutional hepatocytes and/or hepatocellular neoplastic cells. (A glossary of the molecular terms used in this article is given in Table 5.) To understand the correlation between signal intensity in the HB phase and these molecular backgrounds is valuable not only for image interpretation and differential diagnosis among hepatic mass lesions, but also for under-

standing the pathogenesis of benign hepatocellular nodules and its application to personalized medicine.

References

1. Schuhmann-Giampieri G, Schmitt-Willich H, Press WR, Negishi C, Weinmann HJ, Speck U. Preclinical evaluation of Gd-EOB-DTPA as a contrast agent in MR imaging of the hepatobiliary system. Radiology 1992;183(1):59–64.
2. Bluemke DA, Sahani D, Amendola M, et al. Efficacy and safety of MR imaging with liver-specific contrast agent: U.S. multicenter phase III study. Radiology 2005;237(1):89–98.
3. Purysko AS, Remer EM, Veniero JC. Focal liver lesion detection and characterization with Gd-EOB-DTPA. Clin Radiol 2011;66(7):673–684.
4. Di Martino M, Marin D, Guerrisi A, et al. Intraindividual comparison of gadoxetate disodium–enhanced MR imaging and 64-section multidetector CT in the detection of hepatocellular carcinoma in patients with cirrhosis. Radiology 2010;256(3):806–816.
5. Park G, Kim YK, Kim CS, Yu HC, Hwang SB. Diagnostic efficacy of gadoxetic acid-enhanced MRI in the detection of hepatocellular carcinomas: comparison with gadopentetate dimeglumine. Br J Radiol 2010;83(996):1010–1016.
6. Chung YE, Kim MJ, Kim YE, Park MS, Choi JY, Kim KW. Characterization of incidental liver lesions: comparison of multidetector CT versus Gd-EOB-DTPA-enhanced MR imaging. PLoS One 2013;8(6):e66141.
7. Narita M, Hatano E, Arizono S, et al. Expression of OATP1B3 determines uptake of Gd-EOB-DTPA in hepatocellular carcinoma. J Gastroenterol 2009;44(7):793–798.
8. Kitao A, Zen Y, Matsui O, et al. Hepatocellular carcinoma: signal intensity at gadoxetic acid–enhanced MR imaging—correlation with molecular transporters and histopathologic features. Radiology 2010;256(3):817–826.
9. Grazioli L, Bondioni MP, Haradome H, et al. Hepatocellular adenoma and focal nodular hyperplasia: value of gadoxetic acid–enhanced MR imaging in differential diagnosis. Radiology 2012;262(2):520–529.
10. Yoneda N, Matsui O, Kitao A, et al. Beta-catenin-activated hepatocellular adenoma showing hyperintensity on hepatobiliary-phase gadoxetic-enhanced magnetic resonance imaging and overexpression of OATP8. Jpn J Radiol 2012;30(9):777–782.
11. Fukusato T, Soejima Y, Kondo F, et al. Preserved or enhanced OATP1B3 expression in hepatocellular adenoma subtypes with nuclear accumulation of β-catenin. Hepatol Res 2015;45(10):E32–E42.
12. Kitao A, Matsui O, Yoneda N, et al. The uptake transporter OATP8 expression decreases during multistep hepatocarcinogenesis: correlation with gadoxetic acid enhanced MR imaging. Eur Radiol 2011;21(10):2056–2066.
13. Yoneda N, Matsui O, Kitao A, et al. Hepatocyte transporter expression in FNH and FNH-like nodule: correlation with signal intensity on gadoxetic acid enhanced magnetic resonance images. Jpn J Radiol 2012;30(6):499–508.
14. Sekine S, Ogawa R, Ojima H, Kanai Y. Expression of SLCO1B3 is associated with intratumoral cholestasis and CTNNB1 mutations in hepatocellular carcinoma. Cancer Sci 2011;102(9):1742–1747.
15. Kitao A, Matsui O, Yoneda N, et al. Hypervascular hepatocellular carcinoma: correlation between biologic features and signal intensity on gadoxetic acid–enhanced MR images. Radiology 2012;265(3):780–789.
16. Yoneda N, Matsui O, Kitao A, et al. Hypervascular hepatocellular carcinomas showing hyperintensity on hepatobiliary phase of gadoxetic acid-enhanced magnetic resonance imaging: a possible subtype with mature hepatocyte nature. Jpn J Radiol 2013;31(7):480–490.
17. Yamashita T, Kitao A, Matsui O, et al. Gd-EOB-DTPA-enhanced magnetic resonance imaging and alpha-fetoprotein predict prognosis of early-stage hepatocellular carcinoma. Hepatology 2014;60(5):1674–1685.
18. Kitao A, Matsui O, Yoneda N, et al. Hepatocellular carcinoma with β-catenin mutation: imaging and pathologic characteristics. Radiology 2015;275(3):708–717.
19. Bioulac-Sage P, Rebouissou S, Sa Cunha A, et al. Clinical, morphologic, and molecular features defining so-called telangiectatic focal nodular hyperplasias of the liver. Gastroenterology 2005;128(5):1211–1218.
20. Zucman-Rossi J, Jeannot E, Nhieu JT, et al. Genotype-phenotype correlation in hepatocellular adenoma: new classification and relationship with HCC. Hepatology 2006;43(3):515–524.
21. Rebouissou S, Bioulac-Sage P, Zucman-Rossi J. Molecular pathogenesis of focal nodular hyperplasia and hepatocellular adenoma. J Hepatol 2008;48(1):163–170.
22. van Montfoort JE, Stieger B, Meijer DK, Weinmann HJ, Meier PJ, Fattinger KE. Hepatic uptake of the magnetic resonance imaging contrast agent gadoxetate by the organic anion transporting polypeptide Oatp1. J Pharmacol Exp Ther 1999;290(1):153–157.
23. Lorusso V, Pascolo L, Fernetti C, Visigalli M, Anelli P, Tiribelli C. In vitro and in vivo hepatic transport of the magnetic resonance imaging contrast agent B22956/1: role of MRP proteins. Biochem Biophys Res Commun 2002;293(1):100–105.
24. König J, Rost D, Cui Y, Keppler D. Characterization of the human multidrug resistance protein isoform MRP3 localized to the basolateral hepatocyte membrane. Hepatology 1999;29(4):1156–1163.
25. Leonhardt M, Keiser M, Oswald S, et al. Hepatic uptake of the magnetic resonance imaging contrast agent Gd-EOB-DTPA: role of human organic anion transporters. Drug Metab Dispos 2010;38(7):1024–1028.
26. Nassif A, Jia J, Keiser M, et al. Visualization of hepatic uptake transporter function in healthy subjects by using gadoxetic acid–enhanced MR imaging. Radiology 2012;264(3):741–750.
27. Tsuboyama T, Onishi H, Kim T, et al. Hepatocellular carcinoma: hepatocyte-selective enhancement at gadoxetic acid–enhanced MR imaging—correlation with expression of sinusoidal and canalicular transporters and bile accumulation. Radiology 2010;255(3):824–833.
28. Ba-Ssalamah A, Antunes C, Feier D, et al. Morphologic and molecular features of hepatocellular adenoma with gadoxetic acid–enhanced MR imaging. Radiology 2015;277(1):104–113.
29. Benhamouche S, Decaens T, Godard C, et al. Apc tumor suppressor gene is the "zonation-keeper" of mouse liver. Dev Cell 2006;10(6):759–770.
30. Sekine S, Lan BY, Bedolli M, Feng S, Hebrok M. Liver-specific loss of beta-catenin blocks glutamine synthesis pathway activity and cytochrome p450 expression in mice. Hepatology 2006;43(4):817–825.
31. Monga SP. β-catenin signaling and roles in liver homeostasis, injury, and tumorigenesis. Gastroenterology 2015;148(7):1294–1310.
32. Colletti M, Cicchini C, Conigliaro A, et al. Convergence of Wnt signaling on the HNF4alpha-driven transcription in controlling liver zonation. Gastroenterology 2009;137(2):660–672.
33. Lu H, Gonzalez FJ, Klaassen C. Alterations in hepatic mRNA expression of phase II enzymes and xenobiotic transporters after targeted disruption of hepatocyte nuclear factor 4 alpha. Toxicol Sci 2010;118(2):380–390.
34. Nguyen BN, Fléjou JF, Terris B, Belghiti J, Degott C. Focal nodular hyperplasia of the liver: a comprehensive pathologic study of 305 lesions and recognition of new histologic forms. Am J Surg Pathol 1999;23(12):1441–1454.
35. Buscarini E, Danesino C, Plauchu H, et al. High prevalence of hepatic focal nodular hyperplasia in subjects with hereditary hemorrhagic telangiectasia. Ultrasound Med Biol 2004;30(9):1089–1097.
36. De Gaetano AM, Gui B, Macis G, Manfredi R, Di Stasi C. Congenital absence of the portal vein associated with focal nodular hyperplasia in the liver in an adult woman: imaging and review of the literature. Abdom Imaging 2004;29(4):455–459.
37. Mathieu D, Kobeiter H, Maison P, et al. Oral contraceptive use and focal nodular hyperplasia of the liver. Gastroenterology 2000;118(3):560–564.
38. Wanless IR, Mawdsley C, Adams R. On the pathogenesis of focal nodular hyperplasia of the liver. Hepatology 1985;5(6):1194–1200.
39. Bioulac-Sage P, Balabaud C, Bedossa P, et al. Pathological diagnosis of liver cell adenoma and focal nodular hyperplasia: Bordeaux update. J Hepatol 2007;46(3):521–527.

40. Cherqui D, Rahmouni A, Charlotte F, et al. Management of focal nodular hyperplasia and hepatocellular adenoma in young women: a series of 41 patients with clinical, radiological, and pathological correlations. Hepatology 1995;22(6):1674–1681.
41. Chen YW, Jeng YM, Yeh SH, Chen PJ. P53 gene and Wnt signaling in benign neoplasms: beta-catenin mutations in hepatic adenoma but not in focal nodular hyperplasia. Hepatology 2002;36(4 Pt 1):927–935.
42. Bläker H, Sutter C, Kadmon M, et al. Analysis of somatic APC mutations in rare extracolonic tumors of patients with familial adenomatous polyposis coli. Genes Chromosomes Cancer 2004;41(2):93–98.
43. Paradis V, Laurent A, Flejou JF, Vidaud M, Bedossa P. Evidence for the polyclonal nature of focal nodular hyperplasia of the liver by the study of X-chromosome inactivation. Hepatology 1997;26(4):891–895.
44. Rebouissou S, Couchy G, Libbrecht L, et al. The beta-catenin pathway is activated in focal nodular hyperplasia but not in cirrhotic FNH-like nodules. J Hepatol 2008;49(1):61–71.
45. Bioulac-Sage P, Cubel G, Taouji S, et al. Immunohistochemical markers on needle biopsies are helpful for the diagnosis of focal nodular hyperplasia and hepatocellular adenoma subtypes. Am J Surg Pathol 2012;36(11):1691–1699.
46. Fujiwara H, Sekine S, Onaya H, Shimada K, Mikata R, Arai Y. Ring-like enhancement of focal nodular hyperplasia with hepatobiliary-phase Gd-EOB-DTPA-enhanced magnetic resonance imaging: radiological-pathological correlation. Jpn J Radiol 2011;29(10):739–743.
47. Mohajer K, Frydrychowicz A, Robbins JB, Loeffler AG, Reed TD, Reeder SB. Characterization of hepatic adenoma and focal nodular hyperplasia with gadoxetic acid. J Magn Reson Imaging 2012;36(3):686–696.
48. Quaglia A, Tibballs J, Grasso A, et al. Focal nodular hyperplasia-like areas in cirrhosis. Histopathology 2003;42(1):14–21.
49. Nakashima O, Kurogi M, Yamaguchi R, et al. Unique hypervascular nodules in alcoholic liver cirrhosis: identical to focal nodular hyperplasia-like nodules? J Hepatol 2004;41(6):992–998.
50. Kobayashi S, Matsui O, Kamura T, et al. Imaging of benign hypervascular hepatocellular nodules in alcoholic liver cirrhosis: differentiation from hypervascular hepatocellular carcinoma. J Comput Assist Tomogr 2007;31(4):557–563.
51. Sasaki M, Yoneda N, Kitamura S, Sato Y, Nakanuma Y. Characterization of hepatocellular adenoma based on the phenotypic classification: the Kanazawa experience. Hepatol Res 2011;41(10):982–988.
52. Sasaki M, Yoneda N, Kitamura S, Sato Y, Nakanuma Y. A serum amyloid A-positive hepatocellular neoplasm arising in alcoholic cirrhosis: a previously unrecognized type of inflammatory hepatocellular tumor. Mod Pathol 2012;25(12):1584–1593.
53. Sasaki M, Yoneda N, Sawai Y, et al. Clinicopathological characteristics of serum amyloid A-positive hepatocellular neoplasms/nodules arising in alcoholic cirrhosis. Histopathology 2015;66(6):836–845.
54. Calderaro J, Nault JC, Balabaud C, et al. Inflammatory hepatocellular adenomas developed in the setting of chronic liver disease and cirrhosis. Mod Pathol 2016;29(1):43–50.
55. Wanless IR. Micronodular transformation (nodular regenerative hyperplasia) of the liver: a report of 64 cases among 2,500 autopsies and a new classification of benign hepatocellular nodules. Hepatology 1990;11(5):787–797.
56. Reshamwala PA, Kleiner DE, Heller T. Nodular regenerative hyperplasia: not all nodules are created equal. Hepatology 2006;44(1):7–14.
57. Rooks JB, Ory HW, Ishak KG, et al. Epidemiology of hepatocellular adenoma: the role of oral contraceptive use. JAMA 1979;242(7):644–648.
58. Edmondson HA, Henderson B, Benton B. Liver-cell adenomas associated with use of oral contraceptives. N Engl J Med 1976;294(9):470–472.
59. Sale GE, Lerner KG. Multiple tumors after androgen therapy. Arch Pathol Lab Med 1977;101(11):600–603.
60. Sempoux C, Paradis V, Komuta M, et al. Hepatocellular nodules expressing markers of hepatocellular adenomas in Budd-Chiari syndrome and other rare hepatic vascular disorders. J Hepatol 2015;63(5):1173–1180.
61. Lee P, Mather S, Owens C, Leonard J, Dicks-Mireaux C. Hepatic ultrasound findings in the glycogen storage diseases. Br J Radiol 1994;67(803):1062–1066.
62. Labrune P, Trioche P, Duvaltier I, Chevalier P, Odièvre M. Hepatocellular adenomas in glycogen storage disease type I and III: a series of 43 patients and review of the literature. J Pediatr Gastroenterol Nutr 1997;24(3):276–279.
63. Flejou JF, Barge J, Menu Y, et al. Liver adenomatosis: an entity distinct from liver adenoma? Gastroenterology 1985;89(5):1132–1138.
64. Bioulac-Sage P, Rebouissou S, Thomas C, et al. Hepatocellular adenoma subtype classification using molecular markers and immunohistochemistry. Hepatology 2007;46(3):740–748.
65. Bioulac-Sage P, Laumonier H, Couchy G, et al. Hepatocellular adenoma management and phenotypic classification: the Bordeaux experience. Hepatology 2009;50(2):481–489.
66. van Aalten SM, de Man RA, IJzermans JN, Terkivatan T. Systematic review of haemorrhage and rupture of hepatocellular adenomas. Br J Surg 2012;99(7):911–916.
67. Dokmak S, Paradis V, Vilgrain V, et al. A single-center surgical experience of 122 patients with single and multiple hepatocellular adenomas. Gastroenterology 2009;137(5):1698–1705.
68. Cho SW, Marsh JW, Steel J, et al. Surgical management of hepatocellular adenoma: take it or leave it? Ann Surg Oncol 2008;15(10):2795–2803.
69. Courtois G, Morgan JG, Campbell LA, Fourel G, Crabtree GR. Interaction of a liver-specific nuclear factor with the fibrinogen and alpha 1-antitrypsin promoters. Science 1987;238(4827):688–692.
70. Zucman-Rossi J. Genetic alterations in hepatocellular adenomas: recent findings and new challenges. J Hepatol 2004;40(6):1036–1039.
71. Laumonier H, Bioulac-Sage P, Laurent C, Zucman-Rossi J, Balabaud C, Trillaud H. Hepatocellular adenomas: magnetic resonance imaging features as a function of molecular pathological classification. Hepatology 2008;48(3):808–818.
72. van Aalten SM, Thomeer MG, Terkivatan T, et al. Hepatocellular adenomas: correlation of MR imaging findings with pathologic subtype classification. Radiology 2011;261(1):172–181.
73. Ronot M, Bahrami S, Calderaro J, et al. Hepatocellular adenomas: accuracy of magnetic resonance imaging and liver biopsy in subtype classification. Hepatology 2011;53(4):1182–1191.
74. Katabathina VS, Menias CO, Shanbhogue AK, Jagirdar J, Paspulati RM, Prasad SR. Genetics and imaging of hepatocellular adenomas: 2011 update. RadioGraphics 2011;31(6):1529–1543.
75. Rebouissou S, Amessou M, Couchy G, et al. Frequent in-frame somatic deletions activate gp130 in inflammatory hepatocellular tumours. Nature 2009;457(7226):200–204.
76. Pilati C, Amessou M, Bihl MP, et al. Somatic mutations activating STAT3 in human inflammatory hepatocellular adenomas. J Exp Med 2011;208(7):1359–1366.
77. Nault JC, Fabre M, Couchy G, et al. GNAS-activating mutations define a rare subgroup of inflammatory liver tumors characterized by STAT3 activation. J Hepatol 2012;56(1):184–191.
78. Bioulac-Sage P, Balabaud C, Zucman-Rossi J. Subtype classification of hepatocellular adenoma. Dig Surg 2010;27(1):39–45.
79. Agarwal S, Fuentes-Orrego JM, Arnason T, et al. Inflammatory hepatocellular adenomas can mimic focal nodular hyperplasia on gadoxetic acid-enhanced MRI. AJR Am J Roentgenol 2014;203(4):W408–W414.
80. International Working Party. Terminology of nodular hepatocellular lesions. Hepatology 1995;22(3):983–993.
81. Ueda K, Terada T, Nakanuma Y, Matsui O. Vascular supply in adenomatous hyperplasia of the liver and hepatocellular carcinoma: a morphometric study. Hum Pathol 1992;23(6):619–626.